POLAR SEA-ICE CLASSIFICATION USING ENHANCED RESOLUTION NSCAT DATA

Q. P. Remund and D. G. Long
Brigham Young University
459 CB, Provo, UT 84602
801-378-4884, 801-378-6586
remundq@ee.byu.edu, long@ee.byu.edu

M. R. Drinkwater
Jet Propulsion Laboratory
4800 Oak Grove Drive, Pasadena, CA 91109
818-354-8189, 818-354-5473
mrd@pacific.jpl.nasa.gov

Abstract— The NASA scatterometer (NSCAT) collected Ku-band scatterometer measurements from Sept. 1996 to June 1997. These data are converted high resolution six day images of the polar regions through the use of the scatterometer image reconstruction with filter (SIRF) algorithm. SIRF produces images of A and B where A is σ^o at 40° incidence and B is the incidence angle dependence of σ^o. A simple four-dimensional classification technique is proposed which uses the dual polarization parameters A_v, A_h, B_v, and B_h. A k-means clustering classification can be used to separate pixels of the images with differing scattering mechanisms. This method also adapts to the seasonal characteristics of cluster migration by converging to the locally optimal cluster centroids. While validation data was not available at the time of this writing, the method is shown to have high correlation with the NSIDC SSM/I derived multiyear ice maps.

INTRODUCTION

Polar sea ice plays an important role in controlling the global climate. For example, it strongly affects the heat transfer and water exchange cycles. Hence a knowledge of ice thickness and other characteristics is scientifically useful information. Several methods have been employed in the past to classify polar sea ice. Some of these use high resolution SAR data for the classification. These methods have been very successful during certain times of the year when scattering characteristics are most distinct. However, while they yield good classification at high spatial resolution, SAR data has low coverage. Microwave scatterometers, on the other hand, offer regular observations of the polar regions with much broader coverage and multiple incidence angles although the spatial resolution of the measurements are lower.

The NASA scatterometer (NSCAT) is a Ku-band, dual polarization instrument that flew from Sept. 1996 through June 1997. While NSCAT data is no longer available, two more Ku-band scatterometers are slated for launch in late 1998 (QuikSCAT) and early 2000 (Seawinds). Thus, techniques developed for NSCAT data can conceivably be extended to QuikSCAT and Seawinds in the future. The nominal resolution of NSCAT measurements is approximately 25-50 km. However, the scatterometer image reconstruction with filter (SIRF) algorithm can be used to combine 6 days of dual polarization polar measurements to produce images at a spatial resolution of 8-10 km [1]. Over an incidence angle range of 20°-55°, σ^o is essentially a linear function of incidence angle: $\sigma^o = A + B(\theta - 40°)$, where A is σ^o at 40° incidence and B is the incidence angle dependence of σ^o. SIRF produces images of A and B for both vertical and horizontal polarizations. The pixel values of these images are used in the four dimensional classification of ice scattering characteristics.

This paper is organized as follows. Section 2 discusses various ice types and their scattering characteristics. In section 3 the proposed ice classification technique is presented. Section 4 gives the results. The conclusions are given in the final section.

ICE TYPES AND SCATTERING SIGNATURES

Four ice types were chosen for this study: multiyear (MY), rough first year (RFY), smooth first year (SFY), and nilas. Each ice type has characteristic scattering signatures in the four NSCAT parameters. Several factors influence these signatures: surface roughness, salinity (dielectric properties), snow cover, and the distribution of inhomogeneities such as brine pockets [2].

Multiyear ice typically has a very deformed surface with low salinity and low absorptive loss. Volume scattering is characteristic of MY ice as well as rough surface scattering. Consequently, the A values for multiyear ice are very high while the B values are also high (ie. low gradient).

Rough first year ice is well deformed, rough surface ice due to the motion of the ice sheet. High salinity and loss causes the dominant scattering mechanism to be the rough surface, rather than volume scattering. As a result medium to high A and B values are predicted.

Smooth first year ice is generally undeformed, relatively young ice with thicknesses greater than about 60 cm. The high salinity and loss yield medium to low A values and low B values.

Nilas is thin, smooth ice that forms under calm conditions usually in polynyas or open leads. It generally has a short life span due to the deformation induced by wave action. This ice type has very low A and B values.

Scattering signatures of different ice types are most distinct during the winter months. At this time moisture levels in the snow cover on the ice are at a low and snow absorption and scattering become less of a factor. However, as surface temperatures increase and the water content rises, permittivity also increases. This causes the scattering signatures to have more overlap. As a result, ice types

0-7803-4403-0/98/$10.00 © 1998 IEEE

are less distinguishable using microwave data during the warmer seasons. Kwok et al. [3] introduced a seasonally dependent SAR classification technique that uses surface temperature and season information to index a scattering look-up table to compensate for the seasonality of scattering signatures.

NSCAT ICE CLASSIFICATION

For the NSCAT ice classification, the dual polarization A and B images were first ice masked using an NSCAT ice masking algorithm [4]. A pixel by pixel four-dimensional classification is performed using the k-means clustering algorithm [5]. The k-means algorithm requires an initial estimate of the cluster centroid for each ice type. It classifies the pixels using a minimum distance criterion. Once all pixels have been classified, k-means computes the sum of squared distances for each ice type cluster. An iterative process is then followed to optimize the clustering. For each pixel, k-means observes whether moving that pixel to another cluster will decrease the overall sum of squared distances. If it does, the cluster centroids are recomputed as the means of the new clusters. Minimum distance reclassification is performed using these centroids. The algorithm iterates until centroids converge.

The k-means clustering method is desirable for sea ice classification due to the dynamic nature of ice type scattering signatures throughout the year. If the initial cluster centroid estimates are not accurate due to a temporal shift of the centroid, k-means will ideally converge to the true centroid or at least a better estimate of it. Thus, the modified cluster centroids given by k-means for a particular image can be used as the initial cluster centroid estimates for a k-means classification of the next sequential image. Ideally, this process tracks migrating centroids through the four-dimensional parameter space throughout the seasonal cycle.

Since k-means is a minimum distance classifier, if the A and B values are not scaled appropriately, one parameter may be given far more weight in the classification. For this reason, the A and B values are linearly scaled such that both range over approximately 0 to 1 giving equal weight to A and B in the classification. In the SIRF reconstruction the B estimates are inherently more noisy than the A estimates. For this reason, the A values are weighted further by a factor of two making the classification more dependent on A than B. Due to the unavailability of validation data for this experiment, the weightings could not be optimized.

Lack of validation data presents a problem for training the algorithm as well. Without an ice type reference the initial cluster centroid estimates must be based on theory alone. However, in the Arctic, there are regions near the pole that are almost completely MY ice during the winter time. A small region is chosen within the MY portion of the ice sheet. The probability distribution of this region is observed for each parameter. The medians of each of these distributions are used for the initial MY cluster centroid estimates. Similarly, three other regions are chosen from areas that have RFY-like, SFY-like, and nilas-like scattering signatures. The medians used in the cluster centroids estimated from NSCAT data during the period 1997 JD 4-9 are shown in Table 1.

RESULTS

The k-means classification is applied to NSCAT SIRF images from 1997 JD 4-9. The data is first scaled as discussed, then fed into the k-means algorithm. The resulting classified image is shown in Figure 1. Three levels of gray are shown. Very few pixels had nilas-like signatures and are not observable in the figure at the printed scale. While no surface information is available to confirm the RFY, SFY, and nilas classes, the MY location can be compared with the NSIDC SSM/I derived MY ice concentration images. Figure 2 shows the average NSIDC MY ice concentration for 1997 JD 4-9 thresholded at 36%. Clearly, there is a high correlation in the location of NSIDC 36% MY ice and the NSCAT MY ice estimate.

While the RFY, SFY, and nilas classifications remain unvalidated, we can observe the temporal variations of regions classified as these types. Three more NSCAT SIRF image sets were classified using the k-means technique. The imaging periods were 1997 JD 1-6, JD 7-12, and JD 10-15. A selected region around Greenland is displayed for each of these time frames in Figure 3. This time series illustrates that the scattering characteristics being classified have temporal continuity.

CONCLUSIONS

This study shows that NSCAT data is useful in the classification of polar sea ice. A four-dimensional minimum distance classifier is constructed using the enhanced resolution NSCAT A_v, A_h, B_v, and B_h parameters. Data are classified by a k-means clustering algorithm that not only assigns each pixel in the input image to a specific ice type, but iteratively finds the best cluster centroid locations in the minimum sum of squared distances sense. This technique can be used to track dynamic cluster centroids through the seasonal cycle by using the k-means

	MY	RFY-like	SFY-like	Nilas-like
A_v(dB)	-5.14	-14.03	-16.98	-20.97
A_h(dB)	-5.34	-13.76	-16.54	-20.16
B_v(dB/deg)	-0.169	-0.196	-0.238	-0.252
B_h(dB/deg)	-0.146	-0.189	-0.246	-0.258

Table 1: Cluster centroids used in the NSCAT Arctic k-means ice classification experiment.

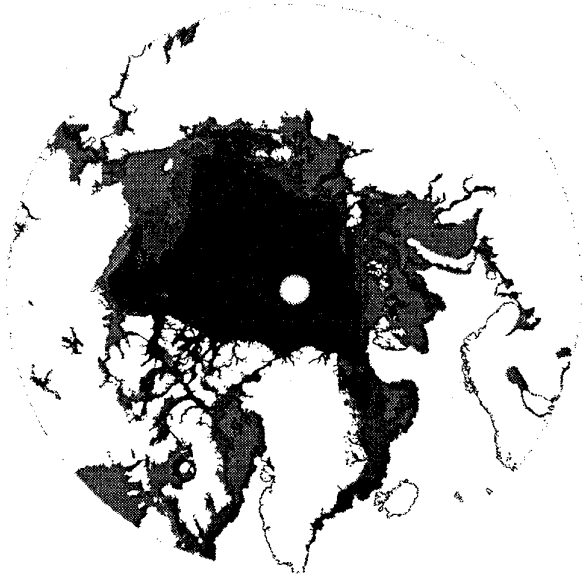

Figure 1: Classified Arctic image using NSCAT data for 1997 JD 4-9. The darkest pixels are MY ice, the medium gray level is RFY-like ice, and the lightest is SFY-like ice. Nilas-like ice doesn't appear at the printed resolution.

cluster centroids from the previous image period for the initial cluster centroid estimates of the current image.

The unavailability of accurate ice type reference data limits the optimization and validation of the algorithm. It is expected that when this data becomes available, the parameters of the algorithm can be tuned to produce the best results possible. Regardless, a high correlation exists between the NSCAT Arctic MY ice map and the NSIDC 36% MY ice map.

REFERENCES

[1] D. Long, P. Hardin, and P. Whiting, "Resolution Enhancement of Spaceborne Scatterometer Data," *IEEE Trans. on Geosci. and Rem. Sens.*, vol. 31, pp. 700–715, 1993.

[2] W.B. Tucker III, D.K. Perovich, and A.J. Gow, "Physical Properties of Sea Ice Relevant to Remote Sensing," in Microwave Remote Sensing of Sea Ice, F.D. Carsey, Ed., Wash. DC: AGU, 1992, pp. 9–28.

[3] R.K. Kwok, E. Rignot, B. Holt, and R. Onstott, "Identification of Sea Ice Types in Spaceborne Synthetic Aperture Radar Data," *J. of Geophys. Res.*, vol. 97, no. C2, pp. 2391–2402, 1992.

[4] Q.P. Remund and D.G. Long, "Automated Antarctic Ice Edge Detection Using NSCAT Data," *Proc. of IGARSS '97*, Singapore, vol. 4, pp. 1841-1843, 1997.

[5] J.A. Hartigan, *Clustering Algorithms*, Wiley, New York, 1975.

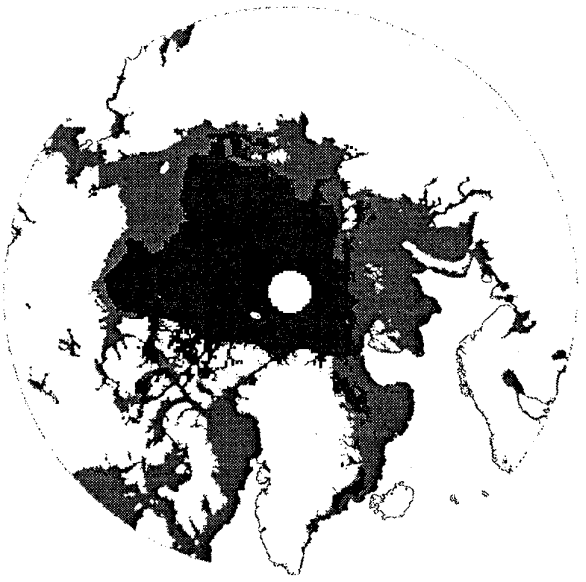

Figure 2: Map of the NSIDC SSM/I derived MY ice concentration over 36%. The black indicates regions with greater than 36% MY ice concentration. The gray simply indicates the rest of the ice extent.

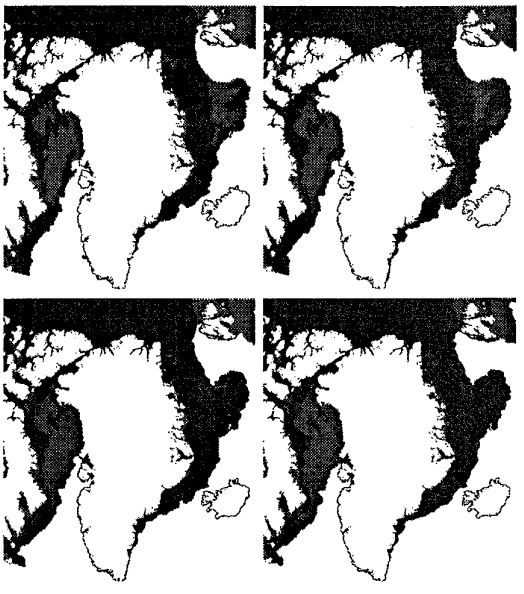

Figure 3: Timeseries of NSCAT ice classified images in the Greenland region. The images are 1997 JD 1-6 (top left), JD 4-9 (top right), JD 7-12 (bottom left), and JD 10-15 (bottom right).